

Strength Reduction in Electrical and Elastic Networks

J.S. Espinoza Ortiz,¹ Chamith S. Rajapakse,¹ and Gemunu H. Gunaratne^{1,2}

¹ *Department of Physics, University of Houston, Houston, TX 77204 and*

² *The Institute of Fundamental Studies, Kandy 20000, Sri Lanka*

Particular aspects of problems ranging from dielectric breakdown to metal insulator transition can be studied using electrical or elastic networks. We present an expression for the mean breakdown strength of such networks. First, we introduce a method to evaluate the redistribution of current due to the removal of a finite number of elements from a hyper-cubic network of conductances. It is used to determine the reduction of breakdown strength due to a fracture of size κ . Numerical analysis is used to show that the analogous reduction due to random removal of elements from electrical and elastic networks follow a similar form. One possible application, namely the use of bone density as a diagnostic tools for osteoporosis, is discussed.

PACS numbers: 87.15.Aa, 87.15.La, 91.60.Ba, 02.60.Cb

I. INTRODUCTION

Networks of electrical or elastic elements are used as models to study phenomena observed in disordered systems. They include dielectric breakdown [1, 2, 3], metal-insulator transitions [4], brittle fracture in disordered solids [5, 6, 7, 8], and strength of trabecular bone [9]. In particular, such models have provided insights on the critical phenomena [10], scale-invariant disorder [3, 10], and size-dependence of the system [11]. In this paper, we will study variations in strength of a class of such systems.

Breakdown processes depend on the size of the longest defect [12, 13, 14] and such extreme value problems are difficult to analyze [10]. However, their statistical properties are expected to be amenable to analysis; this is seen to be the case for the class of problems we study here.

We first consider fused-conducting networks, where the breakdown currents of each element is assumed to be proportional to its conductance; i.e., breakdown of a conductor occurs when the potential difference across it reaches a fixed value. In the simplest case, conductances along each axis of a hyper-cube are set equal. In Section II, we calculate how an external current introduced at a node and removed from an adjacent node is distributed on the network [15, 16]. The Green's Function derived for this case can be used to calculate the current distribution due to an external field on a network from which a finite number of conductances are removed (Section III). This calculation is used to determine how the breaking current on a network of fused conductances is reduced due to a fracture of size κ . The remaining sections of the paper involve numerical analysis to show how this relationship is modified in a variety of other electrical and elastic networks. Section III also provides a discussion of the effects of random removal of elements from a two dimensional network.

In Section IV, we present analogous results for cubic networks with randomly chosen conductances. The relationship between the strength of a network and the fraction of bonds removed is shown to have a form similar to

relationships found in section III. Section V shows that the strength of disordered elastic networks which include elastic and bond-bending energies also follow the same form.

The motivation for this study is to develop a method to relate the mean strength of a bone to its mass [17, 18]. A solution of this problem can provide a non-invasive method to diagnose bone strength and can aid in the management of osteoporosis. These issues are addressed in the concluding section.

II. GREEN'S FUNCTIONS FOR HYPER-CUBIC NETWORK

Consider an infinite, d -dimensional hyper-cubic network where all conductances along the m^{th} direction ($\hat{\mathbf{u}}_m$) are assumed to be equal to σ_m ($m = 1, 2, \dots, d$). In this section, we will calculate the current distribution on this network due to a unit external current introduced at the origin and removed from an adjacent node, say $\mathbf{a} = -\hat{\mathbf{u}}_1$. This result was calculated using a Green's function method by Kirkpatrick [11, 15], and is reproduced here for completeness.

Denote the potential at the node $\mathbf{n} = (n_1, n_2, \dots, n_d)$, by $V(\mathbf{n})$ and the current on the conductor joining nodes \mathbf{n} and $\mathbf{n} + \hat{\mathbf{u}}_m$ by $\mathbf{J}_m(\mathbf{n})$; then,

$$\mathbf{J}_m(\mathbf{n}) = \sigma_m [V(\mathbf{n}) - V(\mathbf{n} + \hat{\mathbf{u}}_m)] . \quad (1)$$

The potentials $V(\mathbf{n})$ can be solved using the Kirchhoff's rules at each node; i.e.,

$$\sum_{m=1}^d \sigma_m \{ [V(\mathbf{n}) - V(\mathbf{n} + \hat{\mathbf{u}}_m)] + [V(\mathbf{n}) - V(\mathbf{n} - \hat{\mathbf{u}}_m)] \} = (\delta_{\mathbf{n},\mathbf{0}} - \delta_{\mathbf{n},\mathbf{a}}) , \quad (2)$$

where the right side is the externally applied current. Eqn. (2) is easily solved by using the Fourier transform $\hat{V}_{\mathbf{k}} = \sum_{\mathbf{n}} e^{-i\mathbf{n} \cdot \mathbf{k}} V_{\mathbf{n}}$, which satisfies

$$\sum_{m=1}^d 2 \sigma_m [1 - \cos(\hat{\mathbf{u}}_m \cdot \mathbf{k})] \hat{V}(\mathbf{k}) = (1 - e^{-i\mathbf{a} \cdot \mathbf{k}}) .$$

Thus

$$\hat{V}(\mathbf{k}) = \frac{(1 - e^{-i\mathbf{a}\mathbf{k}})}{\sum_{m=1}^d 2\sigma_m [1 - \cos(k_m)]}, \quad (3)$$

where $k_m = \hat{\mathbf{u}}_m \cdot \mathbf{k}$. Hence

$$V(\mathbf{n}) = \frac{1/2}{(2\pi)^d} \int_{-\pi}^{\pi} d\mathbf{k} e^{i\mathbf{n}\mathbf{k}} \hat{V}(\mathbf{k}), \quad (4)$$

and

$$\begin{aligned} \mathbf{J}_m(\mathbf{n}) &= \frac{\sigma_m/2}{(2\pi)^d} \int_{-\pi}^{\pi} d\mathbf{k} e^{i\mathbf{n}\mathbf{k}} \\ &\times \frac{(1 - e^{-i\mathbf{k}\mathbf{a}} - e^{ik_m} + e^{i(k_m - \mathbf{k}\mathbf{a})})}{\sum_{m'=1}^d \sigma_{m'} [1 - \cos(k_{m'})]}. \end{aligned} \quad (5)$$

Next we specialize to networks in two dimensions with equal conductances ($\sigma_m = 1$), and define $\alpha(n_x, n_y) \equiv J_y(n_x, n_y)$ and $\beta(n_x, n_y) \equiv J_x(n_x, n_y)$, see Figure 1. The symmetries of the network imply that

$$\begin{aligned} \alpha(n_x, n_y) &= \alpha(-n_x, n_y) = \alpha(n_x, -n_y), \\ \beta(n_x, n_y) &= -\beta(-n_x, n_y) = -\beta(n_x, -n_y). \end{aligned} \quad (6)$$

Combining Eqns. (5) and (6) give

$$\begin{aligned} \alpha(n_x, n_y) &= \frac{2}{\pi^2} \int_0^{\pi} \frac{\cos(n_x k_x) \cos(n_y k_y)}{2 - \cos(k_x) - \cos(k_y)} \sin^2\left(\frac{k_y}{2}\right) d\mathbf{k}, \\ \beta(n_x, n_y) &= \frac{2}{\pi^2} \int_0^{\pi} \frac{\sin[(n_x + \frac{1}{2})k_x] \sin[(n_y + \frac{1}{2})k_y]}{2 - \cos(k_x) - \cos(k_y)} \\ &\times \sin\left(\frac{k_x}{2}\right) \sin\left(\frac{k_y}{2}\right) d\mathbf{k}. \end{aligned} \quad (7)$$

Values of α 's and β 's for several pairs of (n_x, n_y) are presented in tables I and II, and will be used for computation in Section III. Notice that $\alpha(0, 0) = 1/2$, as can be easily confirmed using arguments based on symmetry and superposition [15].

TABLE I: Values of several $\alpha(n_x, n_y)$'s. In particular $\alpha(0, 0) = 1/2$, and $\alpha(1, 0) = 1/2(4/\pi - 1)$.

$\frac{n_y}{n_x}$	0	1	2	3	4	5
0	0.50000	0.13662	0.04648	0.02019	0.01080	0.00670
1	0.13662	0.00001	0.01455	0.01174	0.00816	0.00571
2	0.04648	0.01455	0.00000	0.00404	0.00441	0.00383
3	0.02019	0.01174	0.00404	0.00000	0.00162	0.00208
4	0.01080	0.00816	0.00441	0.00162	0.00000	0.00080
5	0.00670	0.00571	0.00383	0.00208	0.00080	0.00000
6	0.00457	0.00413	0.00314	0.00205	0.00113	0.00045

The α 's and β 's can also be computed perturbatively by expanding the denominator as a series in terms of $(\cos k_x + \cos k_y)/2$. Expansion to fourth order gives values for $\alpha(n_x, n_y)$ and $\beta(n_x, n_y)$ that are accurate to within two percent.

III. RESISTOR NETWORKS IN TWO DIMENSIONS

Consider next, a two dimensional isotropic ($\sigma_x = \sigma_y = 1$) network with an externally applied unit electric field in

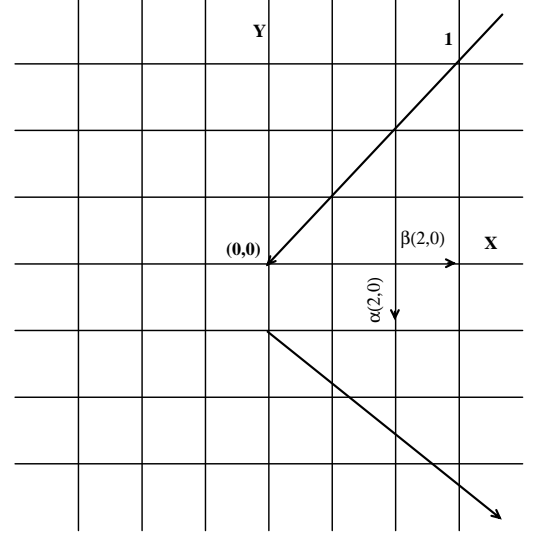


FIG. 1: Scheme to compute the current distribution due to a unit external current introduced at the origin and removed from an adjacent node.

TABLE II: Values of β for the first pairs of (n_x, n_y) .

$\frac{n_y}{n_x}$	0	1	2	3	4	5
0	0.18169	0.04507	0.01315	0.00469	0.00205	0.00106
1	0.04507	0.03052	0.01596	0.00826	0.00451	0.00264
2	0.01315	0.01596	0.01192	0.00789	0.00510	0.00334
3	0.00469	0.00826	0.00789	0.00626	0.00464	0.00337
4	0.00205	0.00451	0.00510	0.00464	0.00384	0.00304
5	0.00106	0.00264	0.00334	0.00337	0.00304	0.00259
6	0.00062	0.00165	0.00225	0.00244	0.00236	0.00214

the y -direction. The currents on this configuration are $J_x(n_x, n_y) = 0$, $J_y(n_x, n_y) = 1$, see Figure 2(a). In this section, we introduce a method to calculate the current distribution on the network when a finite number of conductances are removed. As an application we determine the enhancement of current on the edges of a “fracture” formed by removing κ consecutive conductances.

A. Removal of a Single Conductor

First, we enumerate changes in the current distribution due to the removal of the conductor joining the origin to $(0, -1)$, Figure 2(b). The excess current δ on any remaining element can be considered to be the redistribution of the current that originally passed through the link $(0, 0) - (0, -1)$, see Figure 2(c). δ can be evaluated using the values of $\alpha(m, n)$ and $\beta(m, n)$ by the following procedure. Consider the complete network, with an external current $(1 + J)$ introduced at $(0, 0)$ and removed from $(0, -1)$, as shown in Figure 2(d). $(1 + J)$ is chosen so that a current J passes through $(0, 0) - (0, -1)$, and the remainder ($= 1$) passes through the rest of the

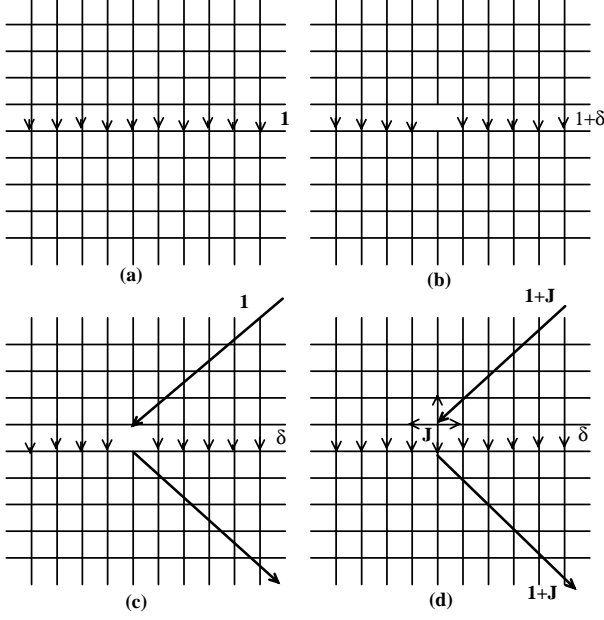


FIG. 2: Scheme to compute the current distribution when a single conductance is removed. In sequence: (a) an isotropic network with a current flow along the y -direction. In (b) a conductance is removed, and δ is the excess of current in any remaining element. Next in (c), a unit external current is introduced in order to compute δ . Finally (d) shows the configuration from which δ can be evaluated.

network; i.e., this second part is the solution to the problem illustrated in Figure 2(c). But from the discussion in section II, the current passing through $(0,0) - (0,-1)$ is $\alpha(0,0) \times (1+J)$. Hence,

$$J = \alpha(0,0) \times (1+J). \quad (8)$$

Since $\alpha(0,0) = 1/2$, we find that $J = 1$ and that the changes of current in the network are given by,

$$\begin{aligned} \Delta J_y(n_x, n_y) &= (1+J)\alpha(n_x, n_y) = 2\alpha(n_x, n_y) \\ \Delta J_x(n_x, n_y) &= (1+J)\beta(n_x, n_y) = 2\beta(n_x, n_y). \end{aligned} \quad (9)$$

In particular, the current on conductances adjacent to that removed in Figure 2(b) is

$$J_{max} = 1 + 2\alpha(1,0) = 4/\pi,$$

as was given by Duxbury et. al. [11].

As a second illustration, we calculate the currents on the network shown in Figure 3(a). As in the first example, the problem can be solved using a complete network on which external currents shown in Figure 3(b) are applied. Notice that prior to removal of the conductances there are no current in AB and hence the current J_1 that is removed at B is required to pass entirely through AB . The currents J_1, J_2, J_3 can thus be obtained from

$$\begin{aligned} J_1 &= \alpha(0,0)J_1 + \beta(0,0)(1+J_2) + \beta(1,0)(1+J_3), \\ J_2 &= \beta(0,0)J_1 + \alpha(0,0)(1+J_2) + \alpha(1,0)(1+J_3), \\ J_3 &= \beta(-1,0)J_1 + \alpha(-1,0)(1+J_2) + \alpha(0,0)(1+J_3). \end{aligned} \quad (10)$$

Notice that the roles of α 's and β 's are reversed when computing the distributions due to the external current J_3 . Solving these equations give $J_1 = 1.50, J_2 = 2.38$, and $J_3 = 2.06$. Some of the currents on this network are given in Figure 3(a), and were confirmed through numerical integrations.

Finally we consider the distribution of current due to a "fracture" of κ consecutive σ_y 's lying along the x -direction, and compute the largest currents (i.e., those on the conductances forming the edges) on the network. Assume that the conductances between $(t,0) - (t,-1)$ where $t = 1, 2, \dots, \kappa$ are removed. This problem is equivalent to having a complete network with currents (J_t+1) introduced at node $(t,0)$ and removed at $(t,-1)$ such that currents J_t pass through links $(t,0) - (t,-1)$. These external currents can be obtained by solving the set of

equations

$$J_t = \sum_{s=1}^{\kappa} \alpha(s-t,0)(J_s+1), \quad (11)$$

and the current on the conductance $(0,0) - (0,-1)$ is given by

$$J_{max}(\kappa) = 1 + \sum_{s=1}^{\kappa} \alpha(s,0)(J_s+1). \quad (12)$$

We have solved Eqns. (11) for values of κ between 1 and 250, and evaluated the maximum current $J_{max}(\kappa)$ on the network using Eqn. (12). Their values as a function of κ are shown by circles in Figure 4. To a very good approximation, J_{max} is given by

$$J_{max}(\kappa) \approx 1 + a_1 \kappa^{1/4} + a_2 \kappa^{1/2}, \quad (13)$$

with $a_1 \approx -0.582$, and $a_2 \approx 0.894$; this expression is shown by the solid line. For $\kappa \gg 1$, this approaches the form $J_{max}(\kappa) = J_0 (1 + a \kappa^{1/2})$, proposed in Ref.[11]. Expressions (11), (12) and (13) were confirmed numerically in a finite network of size $L_x \times L_y (= 100 \times 100)$ centered at the origin. For $\kappa \geq 45$ effects of the boundaries become significant and values of J_{max} near the boundaries are larger than those given by Eqn. (13).

Next, consider a square network of fused conductances; i.e., if the current on an element exceeds I_0 , then it will “burn”, and its conductance would become zero irreversibly. The complete network will fuse when the external field is increased to $E_0 = I_{max}(0) = I_0$, when the current on each element in the y -direction becomes I_0 . The presence of a fracture of length κ will reduce the current $I_{max}(\kappa)$ per link introduced at the top edge of the network. To calculate $I_{max}(\kappa)$, notice that the first elements on the network to burn will be those on the edges of the fracture. As a result κ will increase, and the fracture will propagate in either direction, until the

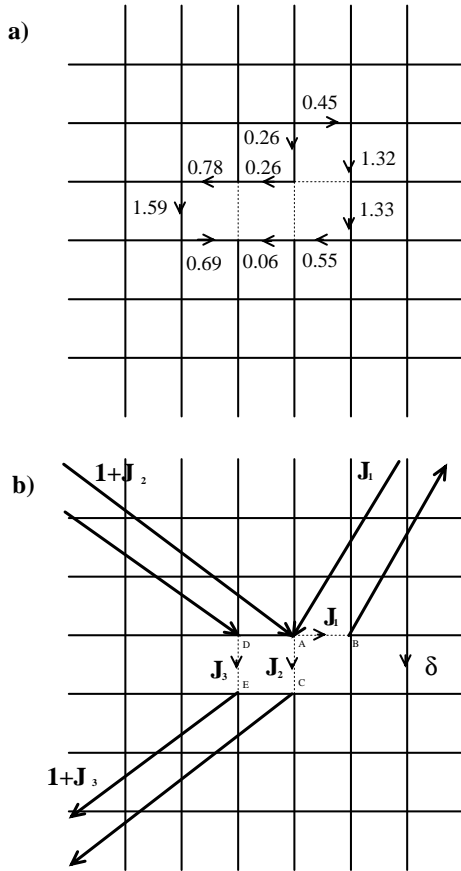


FIG. 3: (a) An isotropic network with the three conductances removed, and current distributions on its boundary. The scheme to compute δ is shown in (b).

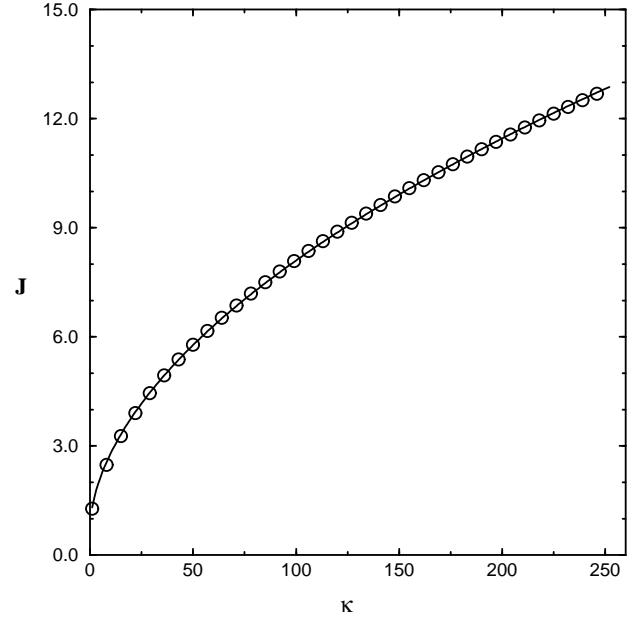


FIG. 4: The largest current distribution resulting from a removal of κ consecutive conductances lying along the x -direction. Results obtained by using Eqns. (11) and (12) are shown by circles, while the expression (13) is shown by continuous line.

network is separated into two segments. From Eqn. (13)

$$\frac{I_{max}(\kappa)}{I_{max}(0)} \approx \frac{1}{1 + a_1 \kappa^\alpha + a_2 \kappa^{2\alpha}}, \quad (14)$$

with $\alpha = 1/4$. In the remainder of this section and the next, we will show through numerical analysis, how this form is modified when resistors are randomly removed from square and cubic networks. Further, the failure strength of random resistors networks and disordered elastic networks will be shown to exhibit a similar form, as long as the networks are not close to the bond percolation threshold.

We also note that the maximum current I_{max} does not necessarily correspond to the first fracture of a conductance in these random cases[11, 19]. However, the yield and ultimate currents have been shown to exhibit similar behavior.

B. Random Removal of Conductances from a Single Layer

Here we consider a finite network of size $L_x \times L_y$ and study the reduction of the maximum current, say $I_{max}(\nu)$, due to the random removal of a fraction ν of conductances on a *single layer* $y = 0$. The length of a largest fracture κ on the layer can be estimated by [11]

$$L_x \nu^\kappa (1 - \nu)^2 \approx 1, \quad (15)$$

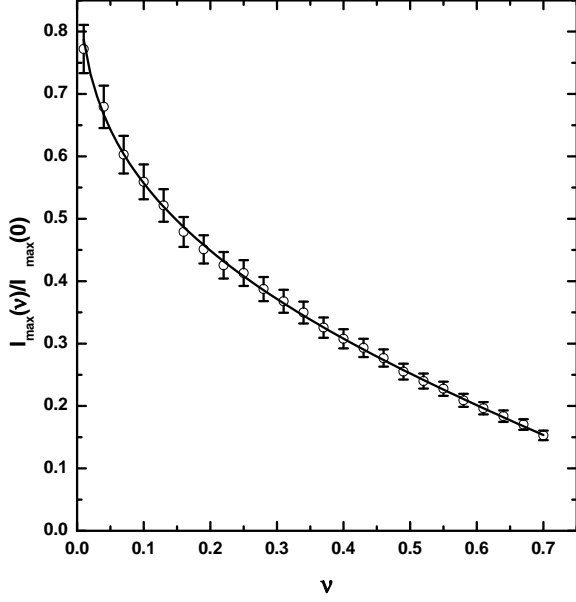


FIG. 5: The reduction of $I_{max}(\nu)$ due to the random removal of a fraction ν of conductances on a single layer $y = 0$ follows Eqn.(17). Here we show the average and the standard error of a set of 100 networks for values of $\nu < 0.70$, with $\alpha \approx 0.37$, $a_1 \approx -0.90$ and $a_2 \approx 1.17$.

where the probability on the left is obtained by requiring the need for κ absent locations (i.e., ν^κ) bounded by two links (i.e., $(1 - \nu)^2$). Thus if $(1 - \nu)^2 \ll L_x$

$$\kappa \approx \frac{\log(L_x)}{\log(1/\nu)}. \quad (16)$$

Assuming a form similar to Eqn. (14),

$$\frac{I_{max}(\nu)}{I_{max}(0)} = \frac{1}{1 + a_1 \left\{ \frac{\log(L_x)}{\log(1/\nu)} \right\}^\alpha + a_2 \left\{ \frac{\log(L_x)}{\log(1/\nu)} \right\}^{2\alpha}}. \quad (17)$$

Figure 5 shows results from computations on a set of 100 networks, for values of $\nu < 0.70$. In these integrations the boundaries at the top and bottom were kept at potentials V_0 and 0, respectively. Had the fractures been independent of each other we would expect $\alpha = 1/4$; the fact that $\alpha \approx 0.37$ suggests a strong correlation between fractures[19].

C. Random Networks in Two Dimensions

We extend the computations of Section IIB to a network of random fused conductors from which a fraction ν of elements have been removed. The conductances are chosen randomly within a range $[1 - \epsilon, 1 + \epsilon]$ and fusing current of each element is assumed to be proportional to its conductance (i.e., they burn when the potential difference between the ends exceed a fixed amount). $I_{max}(\nu)$

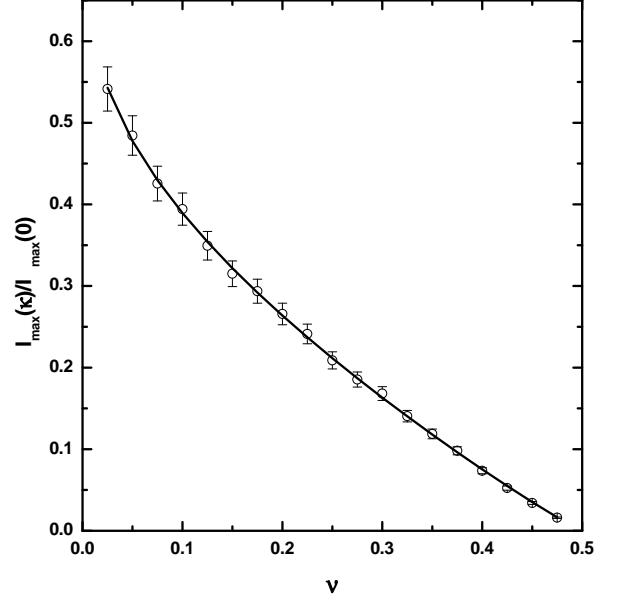


FIG. 6: The reduction of the maximum current as a function of the fraction of conductances removed from a square network. We considered ensembles of 25 networks with size 100×100 . Expression (18) is plotted by continuous line and the average value of $\alpha \approx 0.55$, $a_1 \approx 0.09$ and $a_2 \approx 0.20$.

follows a relationship similar to Eqn. (17) where α depends on ϵ .

Consider first the case $\epsilon = 0$; i.e. all conductances are equal. As the fraction ν of conductances removed reaches the bond percolation threshold $\nu_0 (= 1/2)$, the network separates into multiple segments[20, 21], and hence $I_{max}(\nu_0) \rightarrow 0$. Eqn. (17) fails to satisfy this condition. (Notice that for the quasi-1D case discussed in Section IIB, $\nu_0 = 1$). We propose a modification

$$\frac{I_{max}(\nu)}{I_{max}(0)} = \frac{1}{1 + a_1 \left\{ \frac{\log(N)}{\log(\frac{2N}{\nu})} \right\}^\alpha + a_2 \left\{ \frac{\log(N)}{\log(\frac{2N}{\nu})} \right\}^{2\alpha}}, \quad (18)$$

of Eqn. (17) for this case. Here $N = L_x \times L_y$ is the number of nodes on the network. Figure 6 shows that the mean values (of 25 networks of size 100×100) satisfies Eqn. (18) with a value of $\alpha \approx 0.55$. Including randomness in the conductances changes the value of α , a_1 and a_2 ; but de agreement with Eqn.(18) is equally good.

IV. RESISTOR NETWORKS IN THREE DIMENSIONS

In this section, we discuss the behavior of the breaking strength of cubic networks of fused conductances. Green's function calculations (of Section II) can be used to evaluate the current distributions via $\alpha(n_x, n_y, n_z)$'s and $\beta(n_x, n_y, n_z)$'s. Changes in the current distribution due to the removal of a finite number of conductances can be evaluated using methods outlined in section IIIA.

TABLE III: Values of α 's on the plane $z = 0$, for pairs of (n_x, n_y) .

$\frac{n_x}{n_y}$	0	1	2	3	4	5
0	0.33333	0.06175	0.01392	0.00404	0.00153	0.00073
1	0.06175	0.02323	0.00793	0.00298	0.00130	0.00066
2	0.01392	0.00793	0.00379	0.00184	0.00095	0.00054
3	0.00404	0.00298	0.00184	0.00109	0.00066	0.00041
4	0.00153	0.00130	0.00095	0.00066	0.00045	0.00031
5	0.00073	0.00066	0.00054	0.00041	0.00031	0.00023
6	0.00040	0.00038	0.00033	0.00027	0.00022	0.00017

A. “Penny-Shaped” Fracture

We present the calculation of the current enhancement due to a “penny-shaped” fracture in the $Z = 0$ plane [11, 12], centered at the origin. For a given radius ρ all conductances in the z -direction within a distance ρ of the origin in the $x-y$ plane are removed and changes in the current distribution are computed. This calculation requires evaluating

$$\alpha(n_x, n_y, 0) = \frac{2}{\pi^3} \int_0^\pi \frac{\cos(n_x k_x) \cos(n_y k_y) \sin^2(k_z/2)}{3 - \cos(k_x) - \cos(k_y) - \cos(k_z)} d\mathbf{k} \quad (19)$$

Some values of $\alpha(n_x, n_y, 0)$ are given in TABLE III. The currents on the edge of a fracture can be calculated by methods similar to those in section III. It is found that

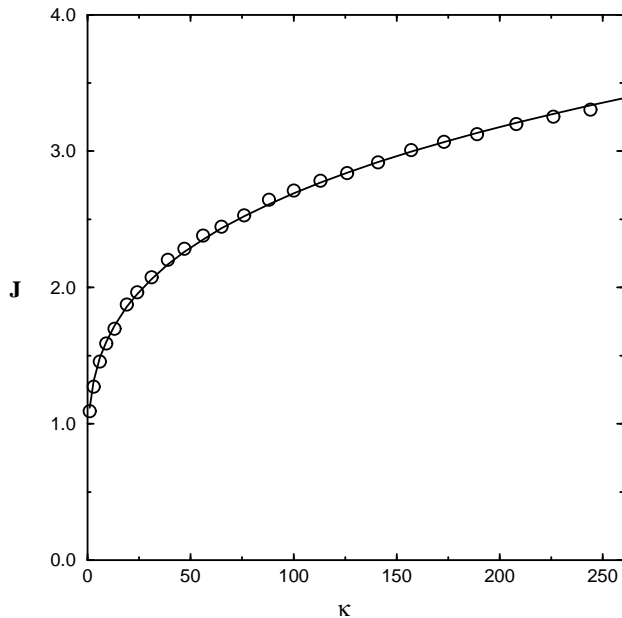


FIG. 7: The largest current resulting from a removal of a “penny shaped” fracture of radius ρ lying on the plane $z = 0$. The calculations using Eqn. (19) are shown by circles, while the expression (20) is shown by the line.

the maximum current for this case is approximately,

$$J_{max}(\kappa) \approx 1 + a_1 \kappa^{1/8} + a_2 \kappa^{1/4}, \quad (20)$$

with $a_1 \approx -0.95$ and $a_2 \approx 1.07$, see Figure 7. Once again these conclusions were checked in numerical integrations on cubic networks of conductances.

B. Random Resistor Networks

In these computations a fraction of conductances from an $L_x \times L_y \times L_z$ network was removed randomly. A potential V_0 was imposed at the top surface of the network, and the bottom surface was grounded. The behavior of the maximum current $I_{max}(\nu)$ for increasing ν is recorded. As in square networks, $I_{max}(\nu)$ is seen to satisfy Eqn. (18), where for cubic networks $\nu_0 \approx 0.7508$ [20, 21]. As before, it is found that α depends on the level ϵ of disorder.

V. ELASTIC NETWORKS

The elastic network model we consider is constructed by displacing the nodes of a hyper-cubic network randomly [9]. The displacements (of less than ϵ) are chosen to be small enough that the topological structure of the network remains unchanged. Adjacent nodes are joined by struts whose elastic moduli are chosen randomly from a pre-determined range; i.e., $k_e \in [k_0(1 - \eta_e), k_0(1 + \eta_e)]$. Bond-bending terms which depend on the variation of the angles between adjacent bonds on the network are included. The linear response coefficients are chosen from within a range $\kappa_b \in [\kappa_0(1 - \eta_b), \kappa_0(1 + \eta_b)]$. These networks are degraded by removing a fraction ν of the links randomly, and the remaining elastic elements are assumed to retain their moduli. Thus the total energy of the network is

$$U = \sum_{\substack{\text{elastic} \\ \text{elements}}} \frac{1}{2} k_e (\delta x)^2 + \sum_{\substack{\text{bonds} \\ \text{angles}}} \frac{1}{2} \kappa_b (\delta \theta)^2$$

where δx is the change of the length of an elastic element under a given external strain of the network, and $\delta \theta$ is the variation of a bond-angle from equilibrium.

A strain based criterion is used to implement fracture of elastic elements and bond angles of the network. Any strut that is strained beyond a value γ is removed from the network along with all bond-angles it contributes to. γ for the elastic elements are chosen from a Weibull distribution whose cumulative density is [12]

$$C(\gamma) = 1 - \exp \left[- \left(\frac{\gamma}{\gamma_c} \right)^m \right]. \quad (21)$$

A corresponding criterion is included for fracture of bonds.

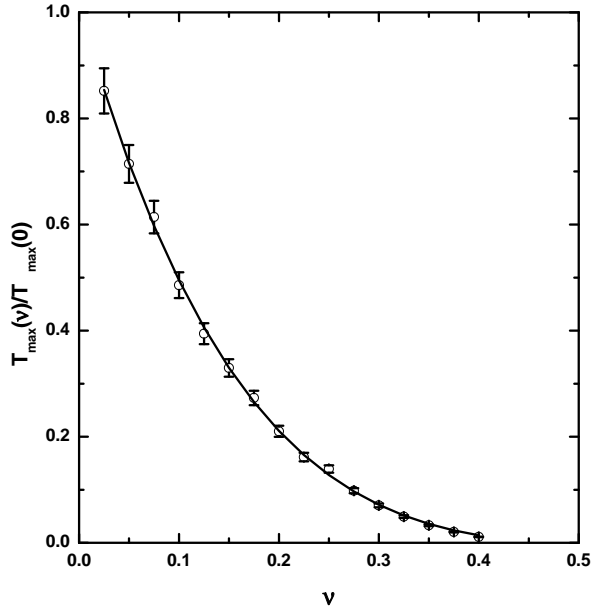


FIG. 8: The reduction of $T_{max}(\nu)$ due to the random removal of a fraction ν of elastic elements. In continuous line is shown the average obeying expression (22) of a square network of size 40×90 . The parameters for the best fit are $\alpha \approx 0.97$, $a_1 \approx -0.11$, $a_2 \approx 0.07$.

A given uniform external strain ζ is imposed through a sequence of small adiabatic increments. If elastic elements or bond-angles are removed from the network due to a fracture, equilibrium is re-calculated prior to increasing ζ . Nodes on the sides of the network transverse to the external strain are constrained to move in plane. The force $T(\zeta)$ required to sustain a strain ζ is calculated by adding the vertical forces on the top of the layer. The equilibrium of a network is calculated by minimizing its energy using the conjugated gradient method [22].

For small values of the compression ζ , the stress-vs-strain relationship $T(\zeta)$ is linear. Numerical analysis shows that $T(\zeta)$ becomes nonlinear (at the yield point) following the first fracture of elastic elements [9]. As ζ is increased further, the stress reaches a maximum (which, for a network a fraction ν of whose elements have been removed, is denoted $T_{max}(\nu)$) prior to failure.

The analog of Eqn. (18) for an elastic network is

$$\frac{T_{max}(\nu)}{T_{max}(0)} = \frac{1}{1 + a_1 \left\{ \frac{\log(N)}{\log(\frac{\nu_0}{\nu})} \right\}^\alpha + a_2 \left\{ \frac{\log(N)}{\log(\frac{\nu_0}{\nu})} \right\}^{2\alpha}}. \quad (22)$$

Figures 8 and 9 show that this expression is satisfied for square and cubic disordered elastic networks. As in elastic networks, α depends on the quantities ϵ , η_e , and η_b characterizing the level of disorder. It is further found to depend on the ratio k_e/κ_b of mean linear response coefficients of elastic and bond-bending terms.

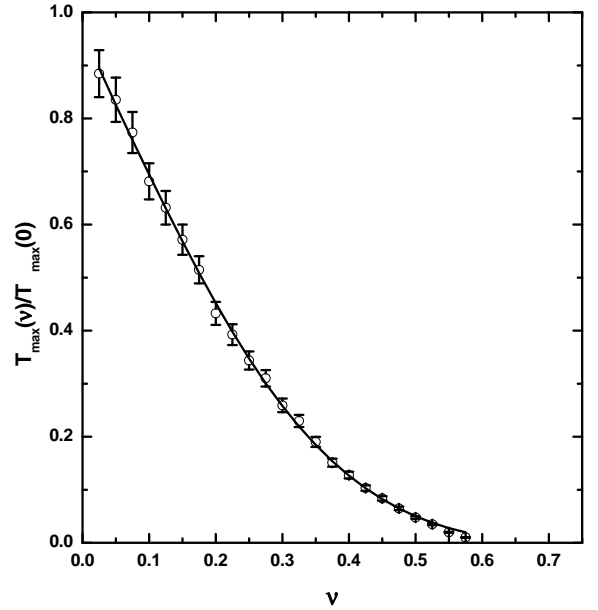


FIG. 9: The same as in Figure 8 for a cubic elastic network of size $20 \times 20 \times 30$. For the nonlinear fit $\alpha \approx 1.14$, $a_1 \approx -0.011$, and $a_2 \approx 0.015$.

VI. DISCUSSIONS AND CONCLUSIONS

The motivation for the work reported here is the need to identify measures that can be used as non-invasive diagnostic tools to estimate the strength of bone. Large bones consist of an outer compact shaft and an inner porous region (trabecular architecture) whose structure is reminiscent of a network of disordered cubic networks [9]. Due to loss of fracture toughness [14] of the outer shaft, the trabecular architecture becomes the principal load carrier in older adults. Reduction in sex-steroid hormones (estrogen and testosterone) effect bone turnover, leading to degradation of the porous bone. Beyond this stage, it is important to monitor the loss of bone strength at regular intervals, preferably with non-invasive diagnosis tools.

The principal mechanism for loss of trabecular mass is through removal of individual struts, due to minor trauma. Fracture toughness and thickness of the remaining trabecular bone do no change appreciably. Mechanical studies on ex-vivo bone samples have shown that trabecular networks from patients with a broad range of ages fracture at a fixed level of strain [23], even though the corresponding fracture stresses exhibit large variations. These observations motivated the fracture criteria used in our models.

Eqn. (18) is the main result of the paper. Its form is justified by the calculations on a network of fused conductors presented in Section IIIA. The numerical analysis of random electrical networks and disordered elastic networks are used to confirm that the strength bears the same relationship to the level of elements removed

from the network. The index α corresponding to random removal of elements is larger than that in the case of a single fracture ($=1/4$), indicating that correlations between fractures is important to determine the strength of a network [19].

It is important to test if samples of trabecular bone satisfy Eqn. (18). Previous studies on bone samples have suggested a nonlinear relationship between the breaking strength (T) and the effective density (ρ) of trabecular bone. It was found heuristically that $T \approx \rho^{-\beta}$, where

$\beta \approx 2.6$. If it is assumed that the density of bone material remains intact and that the fractional reduction of effective density is proportional to ν , then the relationship Eqn. (18) can be tested using this data. Such a comparison will be done in future work.

The authors would like to thank M.Marder, G. Reiter and S.Wimalawansa for discussions. This work is partially funded by the Office of Naval Research, the National Science Foundation and the ICSC - World Laboratory.

-
- [1] H. Takayasu, Phys. Rev. Lett. **54**, 1099 (1985)
 - [2] J.C. Dyre. and Th. Schoder B, Rev. of Modern Phys. **72**, 873 (2000)
 - [3] A. Hansen, E.L. Hinrichsen and S. Roux, Phys. Rev. B **43**, 665 (1991) and in Phys. Rev. Lett. **66**, 2476 (1991)
 - [4] V.K.S. Shante and S. Kirkpatric, Adv. Phys. **20**, 325 (1971)
 - [5] M. Sahimi and J.D. Goddard, Phys. Rev. B **32**, 1869 (1985)
 - [6] J.W. Chung, A. Ross, J. Th. De Hosson and E van der Giessen, Phys. Rev. B **54**, 094 (1996-I)
 - [7] P. Ray and B.K. Chakrabarti, Phys. Rev. B **38**, 715 (1988)
 - [8] Y. Kantor and I. Webman, Phys. Rev. Lett. **52**, 1891 (1984)
 - [9] G.H. Gunaratne, C.S. Rajapakse, K.E. Bassler, K.K. Mohanty and S.J. Wimalawansa, Phys. Rev. Lett. **88**, 68101 (2002)
 - [10] H.J. Herrmann and S. Roux, Phys. Rev. B **39**, 637 (1989)
 - [11] P.M. Duxbury, P.D. Beale and P.L. Leath, Phys. Rev. Lett. **57**, 1052 (1986) and in Phys. Rev. B **36**, 367 (1986)
 - [12] D.G. Harlow and S.L. Phoenix, Int. J. Frac. **17**, 601 (1981)
 - [13] P.L. Leath and P.M. Duxbury, Phys. Rev. B **49**, 14905 (1994)
 - [14] J. Finberg and M. Marder, Phys. Rep. **313**, 1 (1999)
 - [15] S. Kirkpatric, Rev. of Modern Phys. **45**, 574 (1973)
 - [16] J. Bernasconi, Phys. Rev. B **9**, 4575 (1974)
 - [17] Y.C. Fung, "Biomechanics: Mechanical Properties of Living Tissue", Springer-Verlag, New York, 1993
 - [18] K.G. Faulkner, J. Bone. Miner. Res. **15**, 183 (2000)
 - [19] L. De Arcangelis and H.J. Herrmann, Phys. Rev. B **39**, 2678 (1989)
 - [20] J.W. Esam, Rep. Prog. Phys. **43**, 53 (1980)
 - [21] D. Stauffer, "Introduction to Percolation Theory", Taylor & Francis, London Philadelphia, 1985
 - [22] W.H. Press et.al., "Numerical Recipes-The Art of Scientific Computing", Cambridge University Press, Cambridge, 1988
 - [23] H.A. Hogan, S.P. Ruhman and N.H. Sampson, J. Bone Miner. Res. **15**, 284 (2000)
 - [24] E.F. Morgan and T.M. Keaveny, J. Biomech., **34**, 569 (2001)